Rapid deepening of tropical cyclones in the northeastern Tropical Pacific: The relationship with oceanic eddies

Fernando Oropeza* and G. B. Raga

Centro de Ciencias de la Atmosfera
Universidad Nacional Autonoma de Mexico
Mexico City, MEXICO

Date: 17 November, 2010

* Corresponding author: Universidad Nacional Autónoma de México, Ciudad Universitaria, 04510, Mexico City, México, foropeza@atmosfera.unam.mx (F. Oropeza), raga@servidor.unam.mx (G.B. Raga)

ABSTRACT

Several recent studies have documented the importance of anticyclonic ocean eddies in the intensification of tropical cyclones in the Gulf of Mexico and Western North Pacific basins. Studies also indicated the presence of such eddies in the Northeastern Tropical Pacific, mainly during the winter months, but also evident during the tropical cyclone season. In this study, we identify tropical cyclones that experienced rapid and explosive deepening in the northeastern Tropical Pacific during the period: 1993-2008. We evaluate the relative roles of atmospheric parameters and the locally enhanced ocean heat content in the deepening rates of the cyclones.

A total of 233 cyclones were analyzed and the results indicate that in about 90% of the cases there was an interaction between the cyclone and an anticyclonic oceanic eddy. Among those 233 cyclones only forty (17%) experienced *Rapid Deepening* and only nine experienced *Explosive Deepening* (4%). All the cyclones that met the deepening criteria did so after interacting with a region of locally enhanced ocean heat content and 73% reached the threshold deepening rates within an area that we have defined as the Main Favorable Ocean Region (MFOR) in the northeastern Tropical Pacific.

We find that the relative humidity at 550 hPa, and particularly, its integrated value along the vertical in the lower atmosphere play a very important role in the deepening of tropical cyclones in the region, but the most important environmental parameter appears to be the ocean heat content locally enhanced by the presence of anticyclonic eddies.

1. INTRODUCTION

During the 1995 North Atlantic tropical cyclone season, hurricane Opal (the most intense in that season) experienced a sudden and unpredicted intensification 24 h before its landfall. During the rapid deepening from 965 hPa to 916 hPa over 14 h, Opal moved over an Anticyclonic Ocean Eddy (AOE) that had been shed from the Loop Current in the Gulf of Mexico (Hong et al. 2000). After the interaction with the AOE, the 1-min surface winds increased from 35 to more than 60 ms^{-1} and the radius of maximum winds decreased from 40 to 25 km (Shay et al., 2000).

During the 2003 western North Pacific tropical cyclone season, Supertyphoon Maemi (the most intense of the season) intensified (in 1-min sustained wind) from 41 to its peak of 77 ms^{-1} during its 36 h interaction with an AOE. Lin et al. (2005) demonstrated that the AOE acts as an effective insulator between the typhoon and the deeper ocean cold water, inhibiting the effect of the negative feedback between the ocean and the typhoon (originally discussed by Chang and Anthes, 1978).

During the 2005 North Atlantic tropical cyclone season, Katrina and Rita (the third and second most intense cyclones of that season) experienced rapid deepening during their encounter with an AOE in the Gulf of Mexico. Jaimes and Shay (2009) have studied these cases using a variety of datasets to evaluate the rapid increase in intensity observed in Katrina and Rita during their passages over mesoscale ocean features such as an AOE and the Loop Current. They conclude that in each case the decrease in central pressure

correlated better with the depth of the 26°C isotherm and the oceanic heat content than with the sea surface temperature (SST).

The presence of oceanic eddies changes the near surface temperature and vertical structure of the mixed layer, modifying the conditions that represent the energy source for the evolution of tropical cyclone. Figure 1 shows a cartoon of the horizontal and vertical views of the circulation associated with a) an AOE and b) a Cyclonic Ocean Eddy. In the northern hemisphere, anticyclonic horizontal flow induces a secondary circulation directed to the centre of the gyre. In the vertical, this horizontal convergence must be balanced by downward motions. Because the water near the surface is warmer and the secondary downward flow increases the thermocline depth, the result is a local pool of warm water. Such a local pool of warm water could constitute a heat source to hurricanes in the vicinity. These warm features are characterized by a deepening of the isotherms by several meters at the center of the eddy (in regions like the Gulf of Mexico could be several tens of meters) and with different temperature and salinity vertical structure than the surrounding waters. Conversely, an eddy with cyclonic horizontal flow induces a secondary circulation directed to the periphery of the gyre and in the vertical this horizontal divergence must be balanced by upward motion that brings cooler water to the surface, resulting in a local cool pool.

Previous studies (Clarke, 1998; McCreary et al., 1989; Lavin et al., 1992; Giese et al., 1994; Müller-Karger and Fuentes-Yaco, 2000) have shown that the generation of an AOE off the Mexican coast over the Gulf of Tehuantepec (GT) is related to intermittent strong offshore winds in that region, mainly during the boreal cold season (fall–winter). Those winds reach the Pacific Ocean at the GT with gusts of 35 m/s (Romero-Centeno et al.,

2003). Zamudio et al. (2006) analyzed satellite altimeter observations and simulations done with the Naval Research Laboratory Layered Ocean Model to determine the interannual variability of eddies in the GT. Their results suggest that coastally trapped waves, which are generated in the equatorial Pacific, play a crucial role in the modulation and generation of eddies in the GT region and a dominant role in their interannual variability. Furthermore, they showed that AOEs are also present during the tropical cyclone season in that region.

No studies to date have explored the relationship between the presence of AOE in the Northeastern Tropical Pacific (NETP) and tropical cyclones and in particular, we concentrate in this study on the contribution of those eddies to the *Rapid Deepening* of tropical cyclones in the region. We address specifically the following questions:

1. Does the interaction between hurricanes and AOE occur in the NETP basin?
2. Is such an interaction a necessary condition in order for *Rapid* or *Explosive Deepening* to occur during the evolution of tropical cyclones in the region?
3. Is such interaction an important factor in the development of major hurricanes (e.g categories 3, 4 and 5) in the region?

In order to address these questions we will make use of a variety of datasets: i) The best-track information from the National Hurricane Center (NHC) (Davis, et al., 1984); ii) Satellite altimetry products (produced by Ssalto/Duacs and distributed by Aviso with support from Cnes, http://www.aviso.oceanobs.com/duacs/); iii) The North American Regional Reanalysis (NARR), (Mesinger, 2005); iv) the Generalized Digital Environmental Model (GDEM) from U.S. Navy (Teague et al., 1990); v) The World Ocean Atlas (Levitus, 1994); vi) NOAA Optimum Interpolation SST (Reynolds et al., 2002); vii) The SST from

TRMM Microwave Imager (TMI) data (produced by Remote Sensing Systems and sponsored by the NASA Earth Science MEaSUREs DISCOVER Project. Data are available at www.remss.com); and, viii) SST from the Advanced Microwave Scanning Radiometer – EOS (AMSR-E) data (produced by Remote Sensing Systems and sponsored by the NASA Earth Science MEaSUREs DISCOVER Project and the AMSR-E Science Team. Data are available at www.remss.com). The methodology is presented in the following three Sections, describing the selection criteria for rapid and explosive deepening (Section 2), the estimate of the oceanic heat content (Section 3) and the calculation of the atmospheric parameters that contribute to cyclone deepening (Section 4). Section 5 includes the discussion and the evaluation of the relative contribution of mesoscale oceanic features and of atmospheric processes to hurricane intensity fluctuations. Final remarks and conclusions are presented in Section 6.

2. SELECTION OF TROPICAL CYCLONES AS CASE STUDIES

We use the best-track information from the National Hurricane Center (NHC) to identify tropical cyclones that experienced *Rapid Deepening* and/or *Explosive Deepening* in the NETP (1993-2008). The NHC glossary defines the term *Rapid Deepening* (RD) as a decrease in the minimum sea-level pressure of a tropical cyclone of 1.75 hPa/hr or 42 hPa during 24 hours. *Explosive Deepening* (ED) occurs in a cyclone when the central pressure decreases 2.5 hPa/hr for at least twelve hours or 5 hPa/hr for at least six hours.

The deepening rate was estimated from the NHC dataset for each named tropical cyclone between 1993 and 2008. As an example, we present the evolution of central pressure and deepening rate for hurricanes Elida in 2002 (Fig. 2a) and Linda in 1997 (Fig. 2b). From a total number of 233 tropical cyclones, forty (17%) were found to reach the RD criteria and nine (4%) the ED one (Fig. 3). Among the sixteen seasons analyzed, fifteen presented at least one tropical cyclone that reached the Deepening Criteria (DC). The only season that had no tropical cyclone reaching the DC was 1999, the most inactive season *on record* in terms of total number of tropical cyclones, with only eight cyclones. Table I summarizes the cyclones that experienced *Explosive Deepening*, and note that all of them were major hurricanes.

3. INTERACTION OF TROPICAL CYCLONES WITH ANTICLYCLONIC OCEAN EDDIES

3.1 Identifying oceanic eddies in the altimetry data

Satellite altimeter data from Ssalto/Duacs-AVISO is used to detect the presence of an AOE. In particular, the delayed time merged data product from the AVISO project was used, with time resolution of 7 days and grid spacing of 20 arc minutes, and global geographical coverage. The presence of an AOE in the Sea Surface Height Anomaly (SSHA) product is identified by a positive anomaly (dome) and it is possible to calculate its associated surface geostrophic circulation. Figure 4 shows an instantaneous SSHA map and its related geostrophic circulation for 30 May 2007. The presence of four very well defined AOEs in the NETP is clearly visible.

Satellite altimeter data combined with the best track information were used to identify the tropical cyclones that moved close or over an AOE during their evolution. For this study we define a hurricane-AOE interaction as the event where the trajectory of the hurricane at some moment of its evolution goes over an area with a SSHA. Figure 5a shows an interpolated instantaneous SSHA map with the partial trajectory of hurricane Fausto at 0000 UTC 12 September 1996. The figure also shows three panels that correspond to the deepening rate as a function of time and the thresholds for the two deepening criteria (Fig 5b), the evolution of the minimum central pressure (Fig 5c) and the evolution of the SSHA calculated in a square area of 4° by 4° centered on the hurricane current position. Note that in Fig. 5 the hurricane-AOE interaction coincides with the period of *Rapid Deepening*.

We apply this methodology to each of the 233 tropical cyclones observed in the NETP basin from 1993 to 2008, in order to determine which cases presented an interaction with AOEs. The results indicate that for the period considered, about **90%** of the tropical cyclones in this basin presented an interaction with AOEs.

3.2 Estimating the ocean heat content with a two-layer model

While the oceans have been recognized as the energy source for hurricanes for more than half a century (Palmen 1948; Fisher 1958; Perlroth 1967; Leipper 1967), subsequent studies indicated that the maximum hurricane intensity was constrained by thermodynamic effects principally related to the sea surface temperature (SST) (Miller 1958; Emanuel 1986). More recent studies for hurricanes Katrina and Rita (Jaimes and Shay, 2009) showed that decreases of the sea-level pressure were directly correlated to large depth of the 26°C

isotherm and the Ocean Heat Content (OHC), more than with just the SST, which were essentially flat for those cases. The OHC relative to the 26°C isotherm is given by:

$$OHC = \rho_w C_w \int_{Z=H_{26}}^{z=\eta'} (T(z) - 26°C)\partial z \qquad (1)$$

where ρ_w is the average density of the upper ocean water (1026 kgm^{-3}), C_w is the specific heat of seawater at constant pressure (4178 Jkg^{-1}°K^{-1}) and T(z) is the upper ocean temperature structure. Note that the reference temperature is 26°C, since it is the temperature assumed for tropical cyclogenesis (Palmen, 1948) and that the limits of the integral go from the depth of the 26°C isotherm to the elevation of the free-surface.

The estimate of the OHC requires the evaluation of the vertical temperature profile, and we use here the approach proposed by Goni et al. (1996) and Shay et al. (2000). The OHC is estimated using satellite altimetry and SST data in a two-layer reduced-gravity ocean model. In this scheme the upper and lower layers are separated by the depth of the 20°C isotherm and the reduced gravity is given by:

$$g' = \frac{g(\rho_2 - \rho_1)}{\rho_2} \qquad (2)$$

where g is the acceleration of gravity (9.81 ms^{-2}), ρ_1 represents the density of the upper layer and ρ_2 represents the density of the lower layer (O'Brien and Reid, 1967; Kundu, 1990; Goni et al., 1996). In this approach the total depth of the 20°C isotherm is given by:

$$H_{20} = \overline{H}_{20} + \frac{g}{g'}\eta' \qquad (3)$$

where $\overline{H}_{20}$ represents the average depth of the 20°C isotherm from climatology. Mainelli

(2000) proposed that $\overline{H_{20}}$ should be determined only for the tropical cyclone season in the region (May through November) instead of an annual climatology, originally used in the approach of Goni and Trinanes (2003). In Eq. (3), η' is the Sea Surface Height Anomaly (SSHA) from satellite altimetry measurements. The total depth of the 26°C isotherm is determined from the relationship:

$$H_{26} = \frac{\overline{H_{26}}}{\overline{H_{20}}} H_{20} \qquad (4)$$

where $\overline{H_{26}}$ is the average depth of the 26°C isotherm from the climatology determined over the tropical cyclone season only. The OHC is calculated in two stages, depicted schematically in Figure 6. The first stage is determined from the climatological ocean mixed layer depth (*h*), and using the satellite-derived SST as a proxy for the temperature in the mixed layer. The OHC in the mixed layer up to the depth *h* is proportional to *[(SST-26°C) x h]*. The second stage involves estimating the OHC in the layer underneath the mixed layer, from *h* to the depth of 26°C isotherm, and it is approximated as $0.5[H_{26}-h][SST-26°C]$. The total OHC is then estimated as the sum of both contributions. Some underlying assumptions of this approach and detailed evaluation of satellite-inferred values to observed profiles for the Northeastern Tropical Pacific are discussed by Shay and Brewster (2010).

3.3 Application of the two-layer model approach to the case studies

We use the Generalized Digital Environmental Model (GDEM, Version 3.0) climatology (3-D fields of temperature and salinity) from the U.S. Navy, to calculate the climatological values of ρ_1 and ρ_2 along the tropical cyclone season (May through November) using the

CSIRO Matlab seawater library (Morgan and Pender, 1992). We also use GDEM to calculate the depths of the isotherms 20°C and 26°C (figure 7). The climatological depth of the ocean mixed layer was calculated from the World Ocean Atlas (Levitus, 1994).

In order to cover the complete period included in this study (1993-2008), three different sources of satellite-derived SST data were used. For seasons before December 1997, only the NOAA Optimum Interpolation SST data were available, with a one-week temporal resolution and a 1 degree latitude-longitude grid spacing. For seasons between 1998 and 2001, the TRMM Microwave Imager (TMI) data were available daily, with horizontal grid spacing of 0.25^o. The Advanced Microwave Scanning Radiometer –EOS (AMSR-E) data became available in 2002, with daily resolution and horizontal grid spacing of 0.25^o.

The sea surface height anomaly (η') needed for the calculation of the OHC was obtained from the SSalto/DUACS product that changed its periodicity from every 7 days to daily in July 2006, with grid spacing of 20 arc minutes in a global coverage.

All the climatological parameters, SST and SSHA maps used to calculate OHC were objectively analyzed to a regular grid with 0.125^o spacing in latitude-longitude, every 6 hours. This regular grid allows us to determine the time evolution of the average OHC in a 4° by 4° box (as in Marin et al, 2009), centered on the current location of the cyclone for each of the hurricanes considered in our study. Figure 8 shows an example of the instantaneous maps of OHC generated with the described methodology for hurricane Juliette (2001).

4. ATMOSPHERIC ENVIRONMENTAL PARAMETERS

We originally considered the six parameters described by Gray (1975), but our analysis suggested that the most relevant for this study are the following:

1) Vertical shear of the horizontal wind between lower (850 hPa) and upper troposphere (200 hPa)
2) Middle troposphere relative humidity (550 hPa)
3) Vertically integrated relative humidity

These parameters were determined from the publicly-available NARR data that have a grid spacing of 32 km and a time spacing of 3 h, in 29 vertical levels (Mesinger et al., 2005).

The vertical profile of the relative humidity (from 1000 to 550 hPa) was compared with a selected reference value of 75%, in order to estimate its anomaly. As indicated in the example in Figure 9, the positive values (humidity values larger than 75%) and negative values (humidity values smaller than 75%) were determined from the profiles every 6 hours, during the lifetime of all hurricanes in the dataset. An example (Adolph-2001) of this vertical profile and the integrated areas, representing relatively dry (green) and humid (blue) air in the environment surrounding the hurricane system, can be seen in Figure 9.

For all three parameter we calculated the time evolution of the mean value in a 4° by 4° box (as in Marin et al, 2009) centered at the current location of the cyclone, for all the cases considered in the study.

Figure 10 shows the time series for all the environmental parameters for Hurricane Linda in (1997). Note that all the atmospheric parameters were positive: wind shear in the order of

10 ms^{-1}, relative humidity at 550 hPa close to 90% during the entire lifetime of the hurricane, vertically integrated humid air values were around 5000 (corresponding to relative humidity throughout the vertical profile larger than 75%), dry air values around cero (no presence of air with RH smaller than 75% along the vertical profile). The OHC values were the highest in the entire subset of 49 hurricanes that reached the DC (Figure 12-c). Each environmental parameter, both atmospheric and oceanic, was normalized to the highest value presented in all the analyzed cyclones of the dataset in order to compare different cases.

5. DISCUSSION

This study attempts to shed light on the influence of anticyclonic ocean eddies, that locally enhance the oceanic heat content, on the rate of deepening of tropical cyclones in the NETP basin. First, we explore the frequency of interactions between cyclones and AOE: a total of 233 cyclones were analyzed during the period 1993-2008 and the results indicate that such an interaction seems to be widely occurring in the basin, in about 90% of the cases. But is this interaction important for the intensification of the cyclones?

We next determined how frequently cyclones in this basin meet the criteria of *Rapid* or *Explosive Deepening* during their lifetime. Of the total of 233 cyclones only forty (17%) experienced *Rapid Deepening* and only nine exhibited *Explosive Deepening* (4%). Out of the 16 seasons analyzed, in 15 of them there was at least one case. During the 1999 season, none of the eight cyclones that developed met the deepening criteria, this season being the least active on record in terms of number of cyclones (Beven et al., 2004). All cases of

Explosive Deepening became major hurricanes (Table I). As a comparison with the North Atlantic Basin, from a total of 223 cyclones during the same period, forty-five (20%) experienced *Rapid Deepening*, only six (3%) underwent *Explosive Deepening*, and 13out of the 16 seasons analyzed presented at least one case. The three seasons with no cases reaching the deepening criteria were 1993, 1994 and 1997, corresponding to the three least active seasons in the 1993-2008 period, in terms of number of cyclones.

These results suggest that even though the interactions with AOE seem to occur very frequently, only a small fraction experience *Rapid Deepening*. In some cases (such as the one shown in Figure 5), the interaction coincides with the period of *Rapid Deepening* that the cyclone was experiencing with peak intensity reached 6 hours after the interaction. Note that this particular case was intensifying *before* the interaction with the AOE, so the atmospheric conditions were already favorable for intensification.

However, these interactions do not tell the whole story, since the ocean heat content and not the AOE is the relevant parameter for cyclone intensification. The study then focused on the 44 cases that experienced either *Rapid* or *Explosive Deepening* (5 cases of the original 49 were eliminated because they intensified west of 140^{o} W) in order to explore whether their trajectories had been in the vicinity of the regions with locally enhanced ocean heat content during their lifetime. Figures 11 and 12 present a sub-set of four hurricanes that reached the RD and/or ED criteria during its interaction with enhanced OHC related to the presence of an AOE.

5.1 Hurricane Lidia-1993

At 1200 UTC 08 September 1993, the NHC advisory describes a tropical depression that formed about 450 km south of the Gulf of Tehuantepec and reached Tropical Storm intensity by 0000 UTC 09 September 1993, with a wind velocity of 20.5 ms^{-1} and a minimum central pressure of 1003 hPa. As observed in Figure 11b, the atmospheric environment was favorable, having weak vertical wind shear, high values of relative humidity in the middle troposphere and the presence of humid air and no dry air along the vertical. Between 1800 UTC 10 September 1993 and 0600 UTC 11 September 1993, Lidia experienced an episode of *Explosive Deepening* and became a category 4 hurricane, with maximum winds of 66.8 ms^{-1} and minimum central pressure of 930 hPa, as it moved west-northwestward parallel to the southwest coast of Mexico at 4 ms^{-1} over an enhanced OHC region due to the presence of AOE (Fig. 11a). Lidia became the strongest hurricane of that season. Thereafter, Lidia began recurving toward mainland Mexico but it weakened considerably before reaching the coast and landfalling in the Mexican state of Sinaloa. It weakened rapidly over the high terrain of the Sierra Madre Occidental mountain range. It was degraded to a Tropical Depression just after crossing the Mexico-Texas border and dissipated over south-central Texas at 0600 UTC 14 September 1993.

5.2 Hurricane Linda-1997

Hurricane Linda is believed to have originated from an easterly wave observed off the west coast of Africa on 24 August 1997. The wave was tracked across the Atlantic and the Caribbean Sea in satellite imagery by the NHC. Increased cloudiness and convection off the Pacific coast of Panama on 06 September 1997 was likely associated with that wave.

Evidence of a poorly-defined cloud system center within a broad tropical disturbance appeared in satellite imagery early on 9 September. A banded cloud pattern emerged, and the NHC indicates that a Tropical Depression formed from the disturbance around 1200 UTC 9 September 1997 while centered about 740 km south of Manzanillo, Mexico. The tropical cyclone moved northwestward at 2.5 to 5 ms^{-1}, partly in response to a mid- to upper-level low in the vicinity of southern Baja California. Deep convective banding increased and the depression strengthened into Tropical Storm Linda at 0000 UTC 10 September 1997, with maximum winds of 18 ms^{-1} and minimum central pressure of 1005 hPa. As observed in Figure 11d, the atmospheric environment was very favorable for intensification, having weak vertical wind shear, high values of relative humidity in the middle troposphere and no dry air along the vertical profile. Between 0600 UTC 11 September 1997 and 0600 UTC 12 September 1997, Linda experienced an episode of *Explosive Deepening* becoming a category 5 hurricane, with maximum winds of 82.3 ms^{-1} and minimum central pressure of 902 hPa, as it moved over a region of enhanced OHC due to the presence of an AOE (Fig. 11c). Linda became the strongest hurricane ever registered in this basin. It is important to highlight that the values of the locally enhanced OHC that Linda encountered are the highest in our dataset (1993-2008).

5.3 Hurricane Nora-1997

On 18 UTC 16 September 1997, tropical storm Nora was located 463 km southwest of Acapulco, in the Mexican state of Guerrero, with maximum winds of 18 ms^{-1} and minimum central pressure of 1001 hPa. The atmospheric environment was favorable (Fig. 12b), with weak vertical wind shear, high values of relative humidity in the middle troposphere and no

dry air along the vertical profile. By 0000 UTC 21 September 1997, Nora underwent an episode of *Rapid Deepening* becoming a category 4 hurricane, with maximum winds of 59.2 ms^{-1} and minimal central pressure of 950 hPa, as it moved over a region of enhanced OHC due to the presence of an AOE (Fig. 12a). Even though the OHC values were large, the slow translation velocity of Nora (1.4 ms^{-1}) during the first 96 hours clearly forced sea surface cooling. This cooling may have likely been increased by the upwelling and mixing produced by the prior tropical cyclone Linda, that showed a very similar trajectory at the beginning. Linda had interacted with the same region of enhanced OHC a few days before. These factors resulted in a negative feedback that potentially limited Nora maximum intensity (Brand, 1971).

5.4 Hurricane John-2006

On 1200 UTC 28 August 2006, tropical storm John was located 240 km south of the Mexican state of Oaxaca, with maximum winds of 18 ms^{-1} and minimum central pressure of 1004 hPa. The atmospheric environment was favorable for intensification (Fig. 12d), with weak vertical wind shear, high values of relative humidity in the middle troposphere, and no dry air along the vertical profile. By 1800 UTC 29 August 2006, John experienced a *Rapid Deepening* episode becoming a category 2 hurricane. Maximum wind intensity of 48.9 ms^{-1} and minimum central pressure of 965 hPa were observed as John moved parallel to the Pacific coast of Mexico and started to cross over a region of enhanced OHC (Fig. 12c). At 1800 UTC 30 August 2006, John's wind reached a peak intensity of 59.2 ms^{-1} (category 4) and minimal central pressure of 948 hPa, while still over the enhanced OHC region. During its weakening, John encountered another region of enhanced OHC and at

0600 UTC 01 September 2006 experienced another episode of *Rapid Deepening*.

5.5 Hurricane Adrian-1993

So far, we have discussed two cases of *Rapid Deepening* (Nora and John) and two cases of *Explosive Deepening* (Lidia and Linda). Here we present evidence of a case that did not meet neither of DC even though it interacted with a region of enhanced OHC. Figure 13 shows the trajectory and time evolution of the parameters calculated for Adrian, which formed over an area with high values of OHC and moved North-Northwestward. During the first 36 hours, the atmospheric environment was unfavorable for intensification, with high values of wind shear, low values of relative humidity at 550 hPa and dry air along the vertical profile. Clearly, this situation was so unfavorable that Adrian did not experience RD nor ED, and in fact did not develop into a major hurricane. The most important period of deepening during its lifetime is highlighted in Fig. 13b. It is also important to note the impact of dry air towards the end of Adrian's life: even when it was over a favorable OHC region, it weakened quickly due to the intrusion of dry air.

5.6 Main Favorable Ocean Region

All 44 analyzed cases reached the deepening criteria during or after an interaction with a region of locally enhanced OHC related to the presence of an AOE. Figure 14 shows a composite map of the OHC for all the analyzed case studies. We would like to introduce the concept of the *Main Favorable Ocean Region* (MFOR) for the NETP basin (area delimited by the red line in Fig. 14), linked to high values of OHC and limited in latitude by the contour of 17 $KJcm^{-2}$. This value has been identified by Leipper and Volgenau,

(1972) as the amount of heat extracted from the ocean by a passing hurricane for one day. This region is the most probable region for a cyclone to experience RD or ED. In Figure 14, each dot included represents an episode of RD or ED, indicating that 73% of the analyzed cases occurred inside the MFOR. It should be kept in mind that one hurricane can have more than one episode of RD or ED during its lifetime (such as John-2006, seen in Fig. 12). It is also important to note that even though 27% of the cases that experienced RD or ED were outside the MFOR, the majority interacted with regions with OHC values higher than the aforementioned threshold of 17 $KJcm^{-2}$. Recently, Shay and Brewster (2010) introduced the concept of "equivalent OHC" in order to be able to compare basin to basin OHC. This concept incorporates the strength of the thermocline at the bottom of the oceanic mixed layer using a climatological stratification parameter, determined empirically from in situ measurements. They determined this value to range between 1.5 and 3 for NETP, which means that strongly stratified water will act as a barrier to strong shear induced mixing, until the vertical shear decreases the Richardson number below its critical value. The equivalent OHC values in the NETP range then between 25 and 170 $KJcm^{-2}$.

The composite OHC map is now presented in Figure 15 with black dots that correspond to the locations where each of the existing named tropical cyclones in the NHC Best-Track dataset (1949-2008) reached the maximum intensity during their lifetime. Note that 64% of named tropical cyclones in the historic dataset reached their maximum intensity within the MFOR. In Figure 16 the dots indicate the positions where all the existing category 3, 4, and 5 hurricanes in the NHC Best-Track dataset (1949-2008) reached the maximum intensity during their lifetime (differentiated by different colors in the figure). Note that

60% of all major hurricanes reached their maximum intensity within the MFOR.

Beyond the MFOR there is a region with intermediate values of OHC. So if trajectories are in this region, hurricanes may continue their intensification or, at least, extend their lifetime. Once trajectories are outside of this region, the heat content is concentrated in a very shallow layer and the upwelling induced by the hurricane itself brings water from below the thermocline to the surface and leads to weakening. A very clear example of this situation is evident in the case of hurricane Linda (shown in Figures 11c and 11d) as it exits the MFOR and starts to weaken even though the atmospheric factors were still favorable (in particular, the humid air in the vertical column exhibits the highest values of all analyzed cases). When cyclones trajectories stay within the OHC favorable region, it typically leads to intense and long-lived hurricanes, as in the cases of Gilma and John during the 1994 season, with westward trajectories at around 13 and 15N respectively (not shown).

6. CONCLUDING REMARKS

In this study we have defined the Main Favorable Ocean Region (MFOR), a region of very frequent formation and propagation of Anticyclonic Ocean Eddies in the North Eastern Tropical Pacific basin. The MFOR is characterized by high values of Ocean Heat Content, and is delimited by the threshold value around 17 $KJcm^{-2}$.

From our analysis we conclude that even though hurricane-AOE interactions occur in this basin very often (90% of the analyzed cases), only the interactions that take place inside the MFOR are really important for hurricane intensity and lifetime.

All the analyzed cases that met the deepening criteria not only showed interactions with locally enhanced regions of OHC, they also showed favorable atmospheric conditions like low values of wind shear and high values of relative humidity, both in the middle troposphere (550 hPa) and along the profile of lower atmosphere (from 550 to 1000 hPa). The detailed analysis of the environmental parameters for each studied case that met the DC, shows that relative humidity at 550 hPa, and particularly, the integrated value along the vertical profile of the lower atmosphere play a very important role in the deepening of tropical cyclones in the region, but the most important environmental parameter is the available OHC locally enhanced by the presence of AOEs. The heat exchange between the ocean and a hurricane, as it moves over a region of OHC locally enhanced by an AOE, is the most important process leading to *Rapid* and *Explosive Deepening*. We determine that such an interaction is a necessary but not sufficient condition for hurricanes in this basin to experience RD or ED. We also note that the presence of dry air vertically integrated (with relative humidity values smaller that 75%) has a large negative influence on the deepening of tropical cyclones in the region, as was also observed by Marin et al. (2009).

Note that 84% of the hurricanes that experienced RD in the MFOR developed into major hurricanes. Furthermore, when we analyzed the location where all the hurricanes in the full NHC database (1949-2008) reach their maximum intensity, we noted that 64% do it inside the MFOR, and so do 60% of all major hurricanes. Therefore, the interaction is not only important for hurricanes to experience RD or ED, it is also important for reaching their maximum intensities. Linda (1997), the most intense hurricane ever recorded in the NETP

basin had an interaction inside the MFOR with the largest values of OHC observed during the period 1993-2008. This record-setting OHC values were observed in the context of the onset (August) in the NETP of a very strong El Niño year.

The change of tropical cyclone intensity is a complex, nonlinear process that often involves several competing or synergistic factors. Nevertheless, the results presented here strongly suggest that the OHC variability associated with the presence of AOEs in the region, under a favorable atmospheric environment, significantly impact the physical processes controlling cyclone maintenance and intensity change.

7. REFERENCES

Beven, John L., James L. Franklin, 2004: Eastern North Pacific Hurricane Season of 1999. Mon. Wea. Rev., 132, 1036–1047.

Brand, Samson, 1971: The Effects on a Tropical Cyclone of Cooler Surface Waters Due to Upwelling and Mixing Produced by a Prior Tropical Cyclone. J. Appl. Meteor., 10, 865–874.

Chang, S. and R. Anthes, 1978: Numerical simulations of the ocean's nonlinear baroclinic response to translating hurricanes. J. Phys. Oceanogr., 8, 468–480.

Clarke, A. J., 1998: Inertial wind path and sea surface temperature patterns near the Gulf of Tehuantepec and Gulf of Papagayo, J. Geophys. Res., 93, 15,491– 15,501.

Davis, M. A. S., G. M. Brown, and P. Leftwich, 1984: A Tropical Cyclone Data Tape for the Eastern and Central North Pacific Basins, 1949-1983: Contents, Limitations, and Uses. NOAA Technical Memorandum NWS NHC 25, Coral Gables, Florida.

Emanuel, K A., 1986: An air-sea interaction theory for tropical cyclones Part 1: Steady-State maintenance. J. Atmos. Sci., 43, 585-605.

Fisher, E. L., 1958: Hurricanes and the sea-surface temperature field. J. Meteor., 15, 328-333.

Giese, B. S., J. A. Carton, and L. J. Holl, 1994: Sea level variability in the eastern tropical Pacific as observed by TOPEX and Tropical Ocean-Global Atmosphere Tropical Atmosphere-Ocean Experiment, J. Geophys. Res., 99, 24,739–24,748.

Goni, G. J., and J. Trinanes, 2003: Ocean thermal structure monitoring could aid in the intensity forecast of tropical cyclones. EOS, Trans. Amer. Geophys. Union, 85, 179

Goni, G. J., S. Kamholz, S. L. Garzoli, and D. B. Olson, 1996: Dynamics of the Brazil/Malvinas confluence based on inverted echo sounders and altimetry. J. Geophys. Res., 95, 22103-22120.

Gray, W. M., 1975: Tropical Cyclone genesis. Dept. of Atmos. Sci. Paper No. 234, Colorado State Univ., Ft. Collins, CO.

Hong, X., S. W. Chang, S. Raman, L. K. Shay, and R. Hodur, 2000: The interaction between Hurricane Opal (1995) and a warm core ring in the Gulf of Mexico. Mon. Wea. Rev., 128, 1347–1365.

Jaimes, Benjamin, Lynn K. Shay, 2009: Mixed Layer Cooling in Mesoscale Oceanic Eddies during Hurricanes Katrina and Rita. Mon. Wea. Rev., 137, 4188–4207.

Kundu, P. K., 1990: Fluid Mechanics, Academic Press International, 253 pp.

Lavín, M. F., J. M. Robles, M. L. Argote, E. D. Barton, R. Smith, J. Brown, M. Kosro, A. Trasviña, H. S. Vélez Muñoz, and J. García, 1992: Física del Golfo de Tehuantepec, Rev. Cienc. Desarrollo, XVIII, 97– 108.

Leipper, D. F., 1967: Observed oceanic conditions and hurricane Hilda, 1964. J Atmos. Sci., 24, 182-196.

Leipper, D. and D. Volgenau, 1972: Hurricane heat potential of the Gulf of Mexico. J. Phys. Oceanogr., 2, 218‑224.

Levitus, S. and T.P. Boyer. World Ocean Atlas 1994 Volume 4: Temperature, number 4, 1994.

Lin, I-I, C. C. Wu, K. A. Emanuel, I. H. Lee, C. R. Wu, and I. F. Pun, 2005: The interaction of Supertyphoon Maemi (2003) with a warm ocean eddy. Mon. Wea. Rev., 133, 2635–2649.

Mainelli, M. M., 2000: On the role of the upper ocean in tropical cyclone intensity change. M.S. Thesis, University of Miami, Miami, FL, 73 pp.

Marin, J., D. Raymond, and G. Raga, 2009: Intensification of tropical cyclones in the GFS model. Atmos. Chem. Phys., 9, 1407–1417.

McCreary, J. P., Jr., H. S. Lee, and D. B. Enfield, 1989: The response of the coastal ocean to strong offshore winds: With application to the Gulfs of Tehuantepec and Papagayo, J. Mar. Res., 47, 81–109.

Mesinger, F.; G. DiMego, E. Kalnay, K. Mitchell, P.C. Shafran, W. Ebisuzaky, D. Jovic, J. Woollen, E. Rogers, E.H. Berbery, M.B. Ek, Y. Fan, R. Grumbine, W. Higgins, H. Li, Y. Lin, G. Manikin, D. Parrish and W. Shei, 2005: North American Regional Reanalysis. BAMS, 87:3, 343-360.

Miller, B. I., 1958: On the maximum intensity of hurricanes. J. Meteor.,15, 184–195.

Müller-Karger, F. E., and C. Fuentes-Yaco, 2000: Characteristics of wind generated rings in the eastern tropical Pacific Ocean, J. Geophys. Res., 105, 1271–1284.

O'Brien, J. J. and R. O. Reid, 1967: The non-linear response of a two-layer ocean to a stationary axiallysymmetric hurricane: Part I Upwelling induced by momentum transfer. J. Atmos. Sci., 24, 205-215

Palmen, E., 1948: On the formation and structure of tropical cyclones. Geophysica, 3, 26-38.

Perlroth, I., 1967: Hurricane behavior as related to oceanographic environmental conditions. Tellus, 19, 258-268.

Reynolds, R. W., N. A. Rayner, T. M. Smith, D. C. Stokes and W. Wang, 2002: An improved in situ and satellite SST analysis for climate. J. Climate, 15, 1609-1625.

Romero-Centeno, R., J. Zavala-Hidalgo, A. Gallegos, and J. J. O'Brien, 2003: Tehuantepec isthmus wind climatology and ENSO signal, J. Clim., 16, 2628– 2639.

Shay, Lynn K., Jodi K. Brewster, 2010: Oceanic Heat Content Variability in the Eastern Pacific Ocean for Hurricane Intensity Forecasting. Mon. Wea. Rev., 138, 2110–2131.

Shay, L. K., G. J. Goni, and P. G. Black, 2000: Effects of a warm oceanic feature on Hurricane Opal. Mon. Wea. Rev., 128, 1366–1383.

Teague, W.J., M.J. Carron, and P.J. Hogan, 1990: A comparison between the Generalized Digital Environmental Model and Levitus climatologies. J. Geophys. Res., 95, 7167-7183.

Zamudio, L., H. E. Hurlburt, E. J. Metzger, S. L. Morey, J. J. O'Brien, C. E. Tilburg, and J. Zavala-Hidalgo, 2006: Interannual variability of Tehuantepec eddies, J. Geophys. Res., 111, C05001, doi:10.1029/2005JC003182.

TABLE I: Hurricanes that experienced Explosive Deepening in the northeastern Tropical Pacific basin in the period 1993-2008.

Name	Season	Comments
Kenneth	1993	Category 4, second most intense of the season
Lidia	1993	Category 4, third most intense of the season
Linda	1997	Category 5, most intense ever in the basin
Carlotta	2000	Category 4, most intense of the season
Juliette	2001	Category 4, most intense of the season
Elida	2002	Category 5, third most intense of the season
Kenna	2002	Category 5, most intense of the season
Howard	2004	Category 4, second most intense of the season
Ioke	2006	Category 5, most intense of the season (formed west of 140 W)

FIGURES

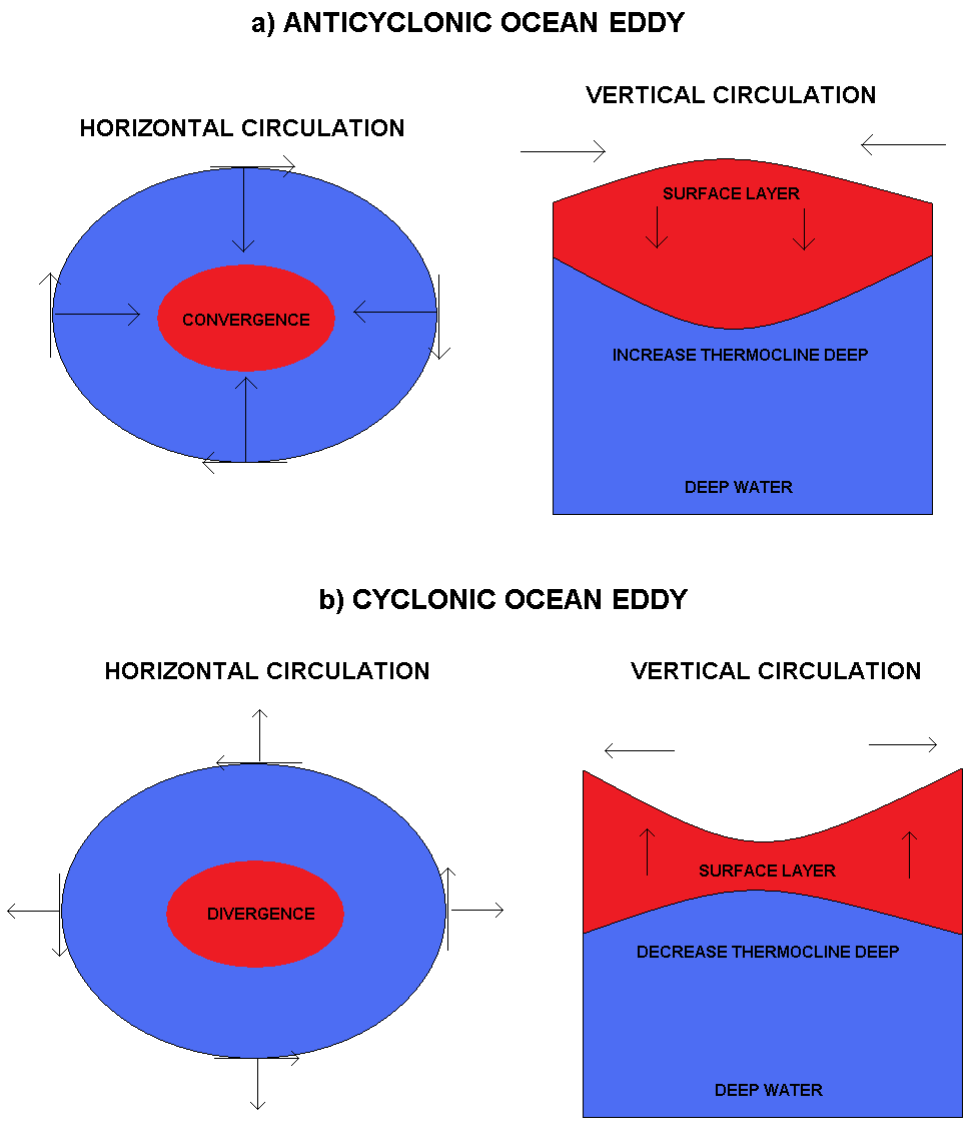

Figure 1: Horizontal and vertical views of a sketched internal dynamics of a) Anticyclonic Ocean Eddy and b) Cyclonic Ocean Eddy in the northern hemisphere.

a)

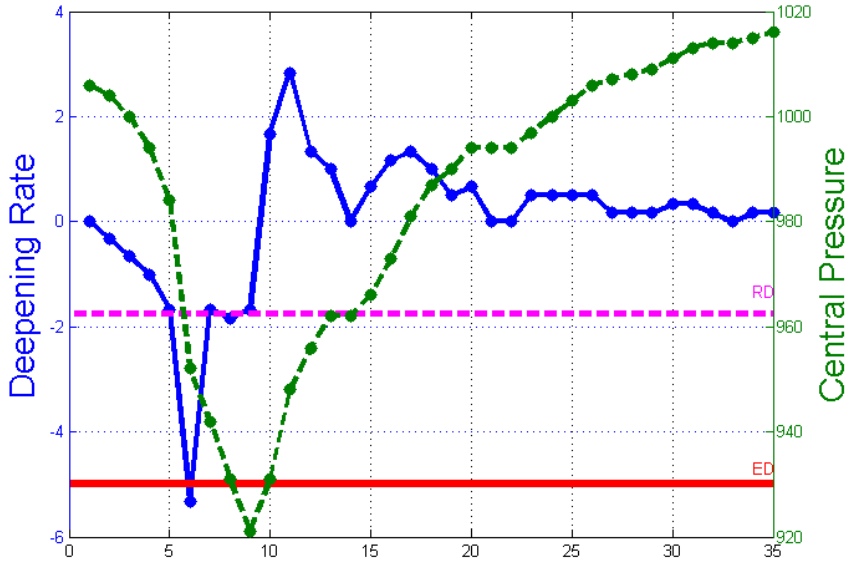

b)

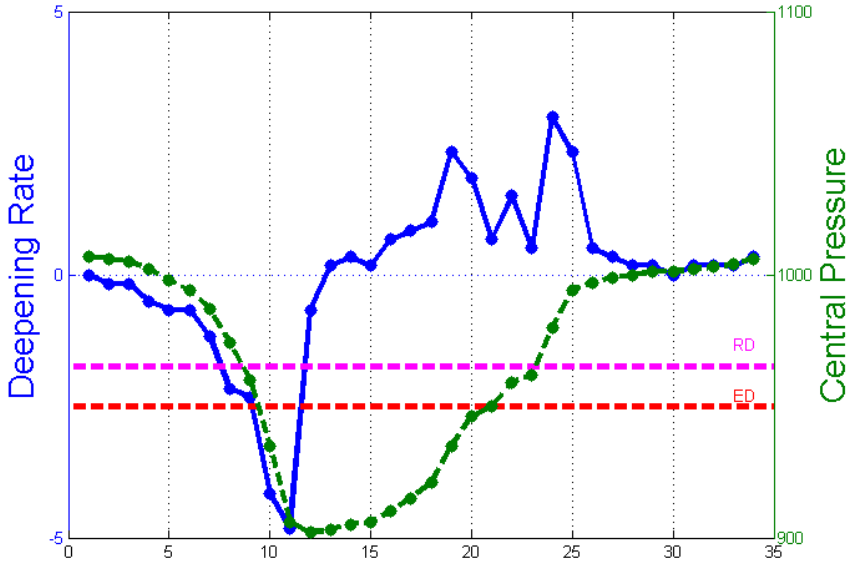

Figure 2: Central pressure (dashed green line, right size scale) and deepening rate (solid blue line, left size scale) evolution for tropical cyclones a) Elida-2002 and b) Linda-1997. The dashed magenta horizontal line is indicating the RD criteria threshold (1.75 hPa/h), the dashed horizontal red line (in b) is indicating ED criteria threshold (2.5 hpa/h for at least 12 hrs) and the solid horizontal red line (in a) de ED criteria threshold (5 hPa/h for at least 6 hrs).

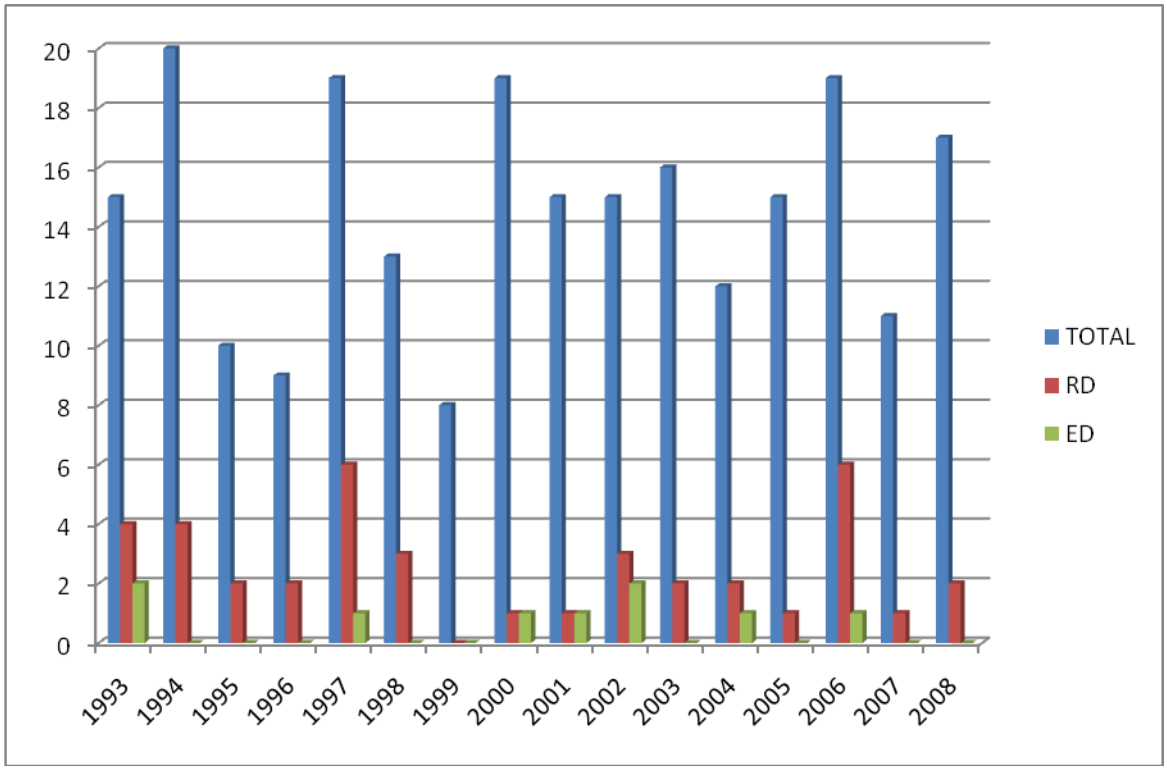

Figure 3: Frequency distribution of total number of tropical cyclones (233 in blue), number of tropical cyclones reaching the RD criteria (40 in red), number of tropical cyclones reaching the ED criteria (9 in green).

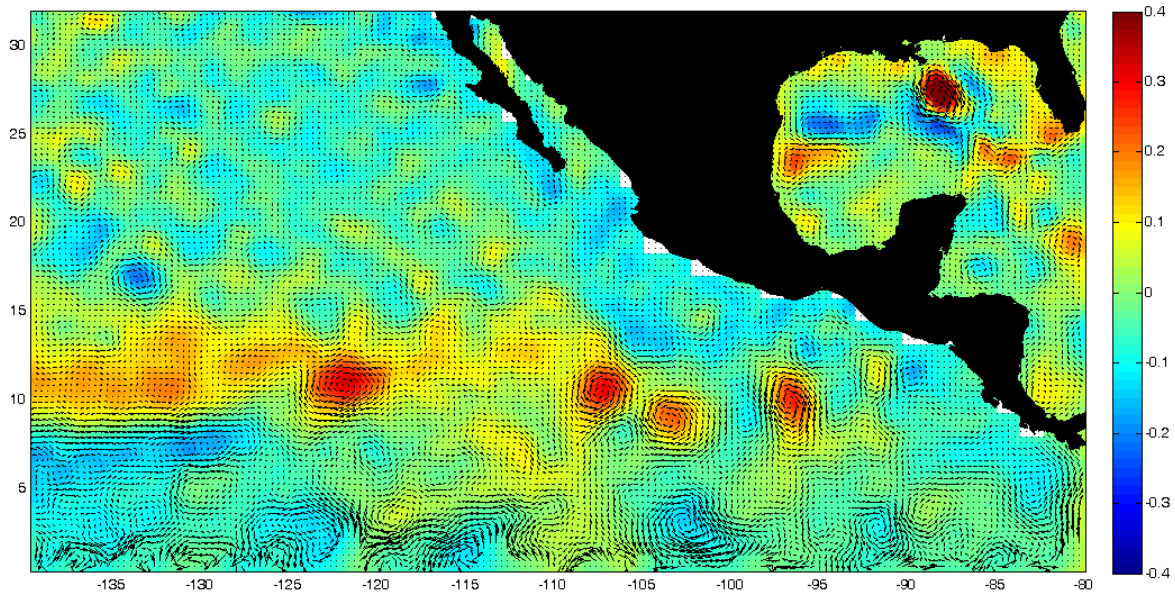

Figure 4: SSH anomaly (m) from AVISO and their associated surface geostrophic circulation for 30 May 2007, showing four very well developed Anticyclonic Ocean Eddies at (10N, 95W), (9N, 103W), (11N, 107W), and (11N, 123W).

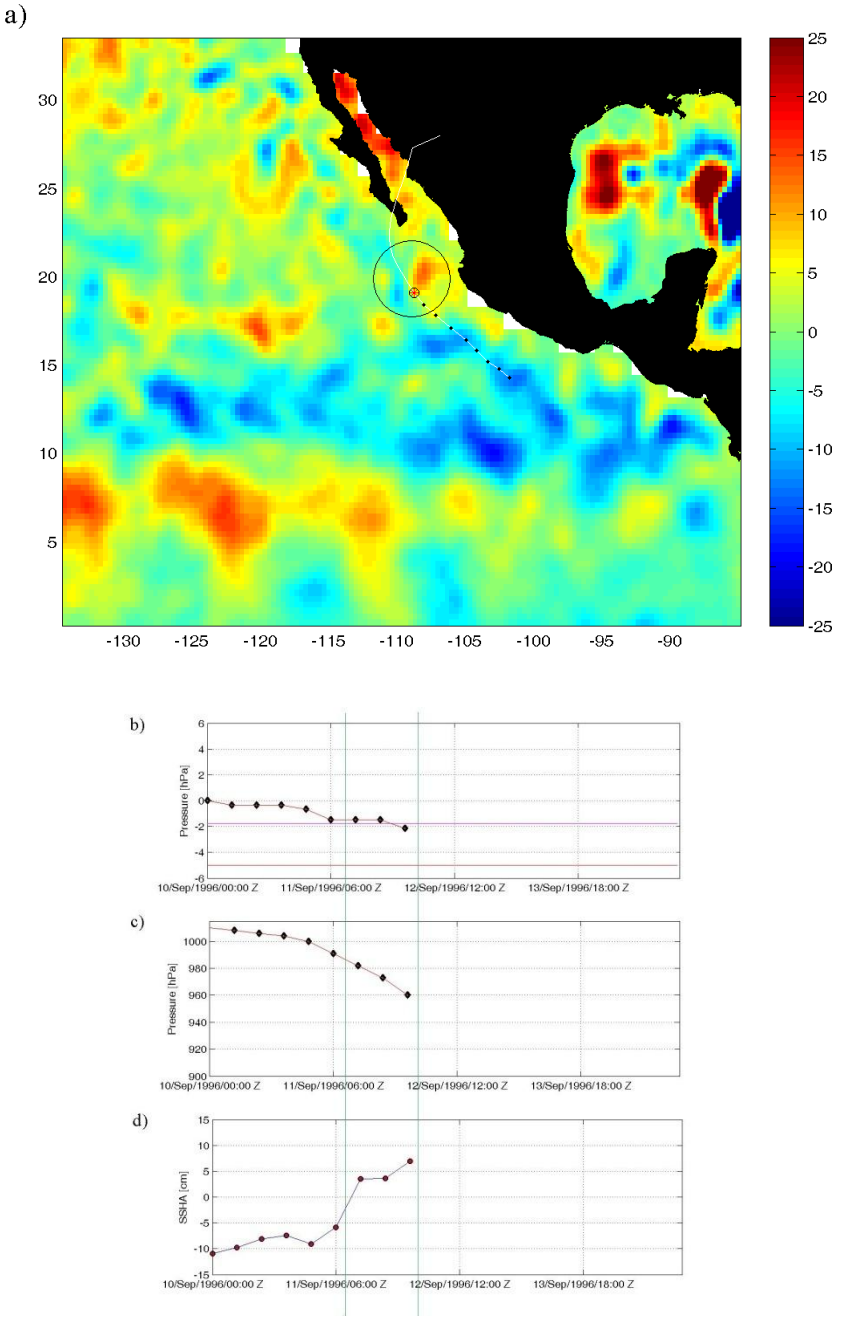

Figure 5: a) SSHA instant map (cm) objectively analyzed from AVISO for 0000 UTC 12 September 1996 and partial Best-Track trajectory for hurricane Fausto for the same date, b) deepening rate (dp/dt) evolution, the magenta horizontal line indicates the threshold for Rapid Deepening Criteria and the horizontal red line indicates the threshold for Explosive Deepening Criteria, c) Minimum central pressure evolution, d) Sea Surface Height Anomaly evolution calculated from objectively analyzed maps for each Best-Track hurricane position. Circle in the map (a) and vertical green lines in the time series (b,c and d), highlight the moment of hurricane-AOE interaction.

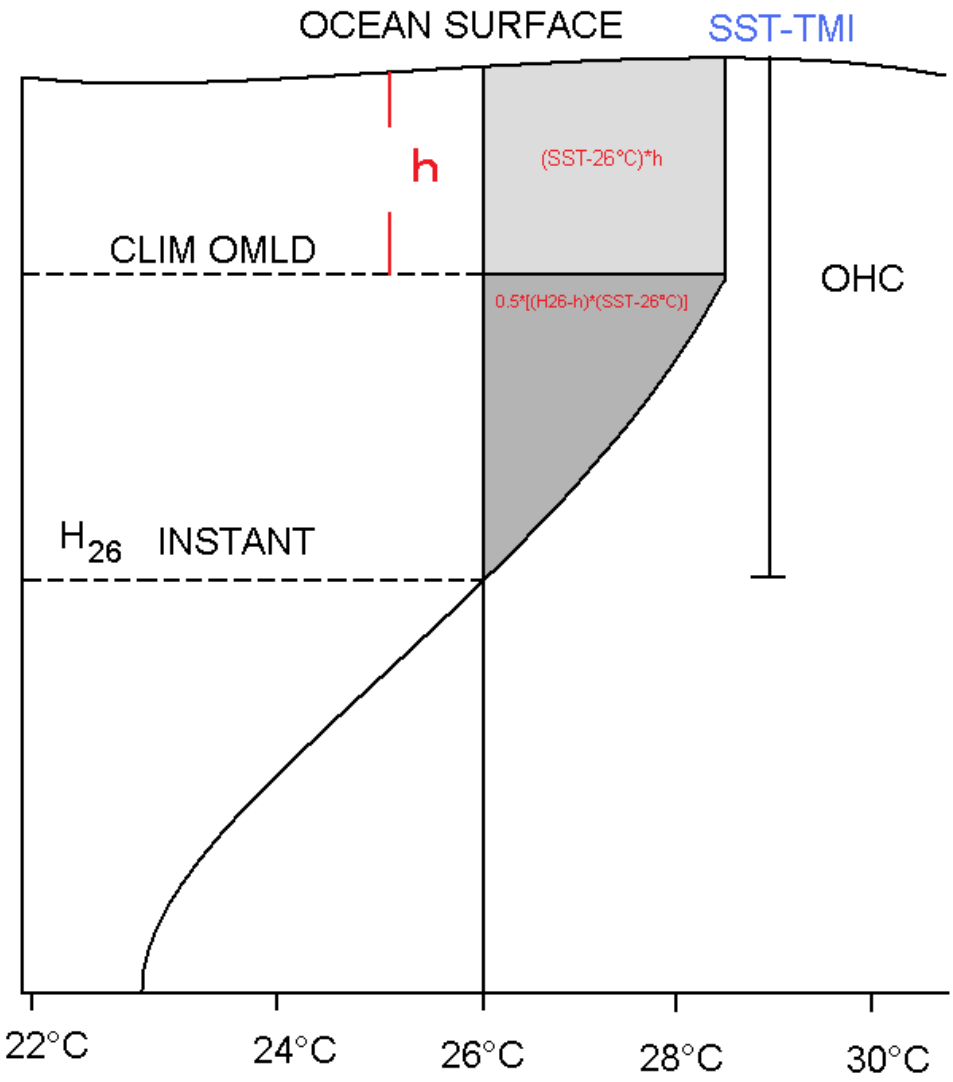

Figure 6: Schematic description of the Ocean Heat Content calculation using the two-layer model approach

a) SST (°C)

b) Salinity (psu)

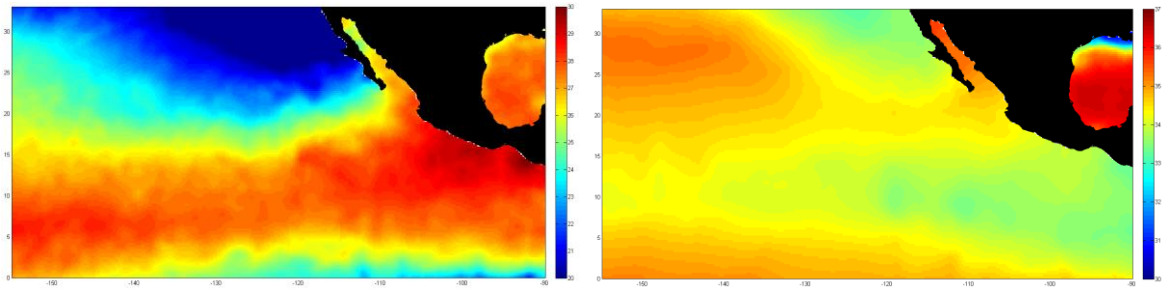

c) ρ_1 (Kgm^{-3})

d) ρ_2 (Kgm^{-3})

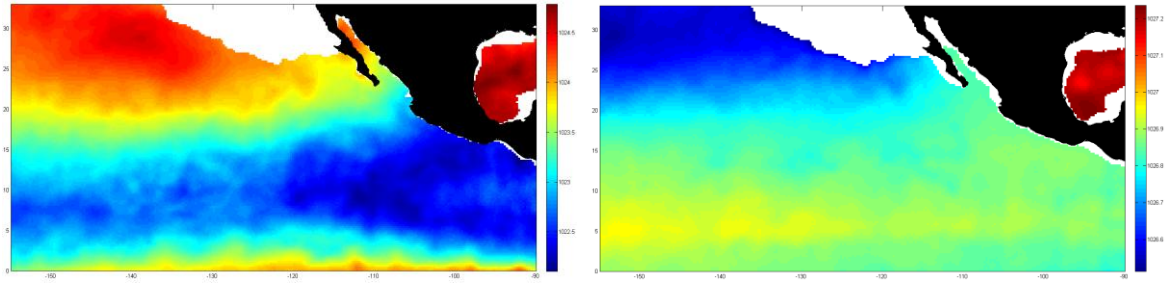

e) H_{20} (m)

f) H_{26} (m)

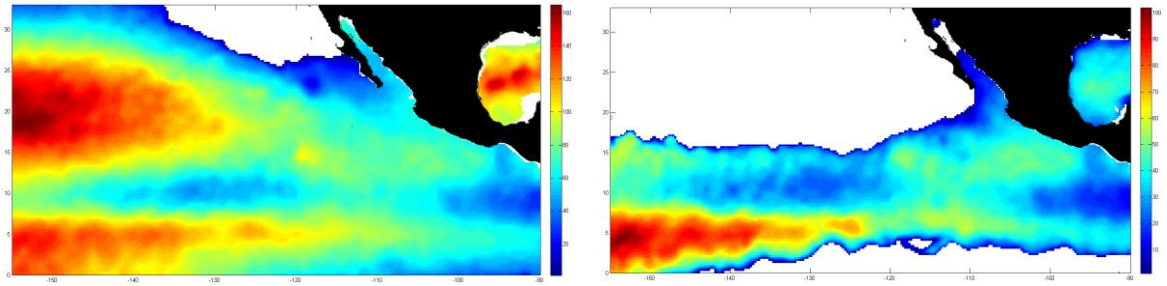

Figure 7: Generalized Digital Environmental Model (GDEM) derived hurricane-seasonal climatology values for a) SST (°C), b) Salinity (psu), c) potential density of the upper layer (Kgm^{-3}), d) potential density of the lower layer (kgm^{-3}), e) depth of the 20°C isotherm and f) depth of the 26°C isotherm.

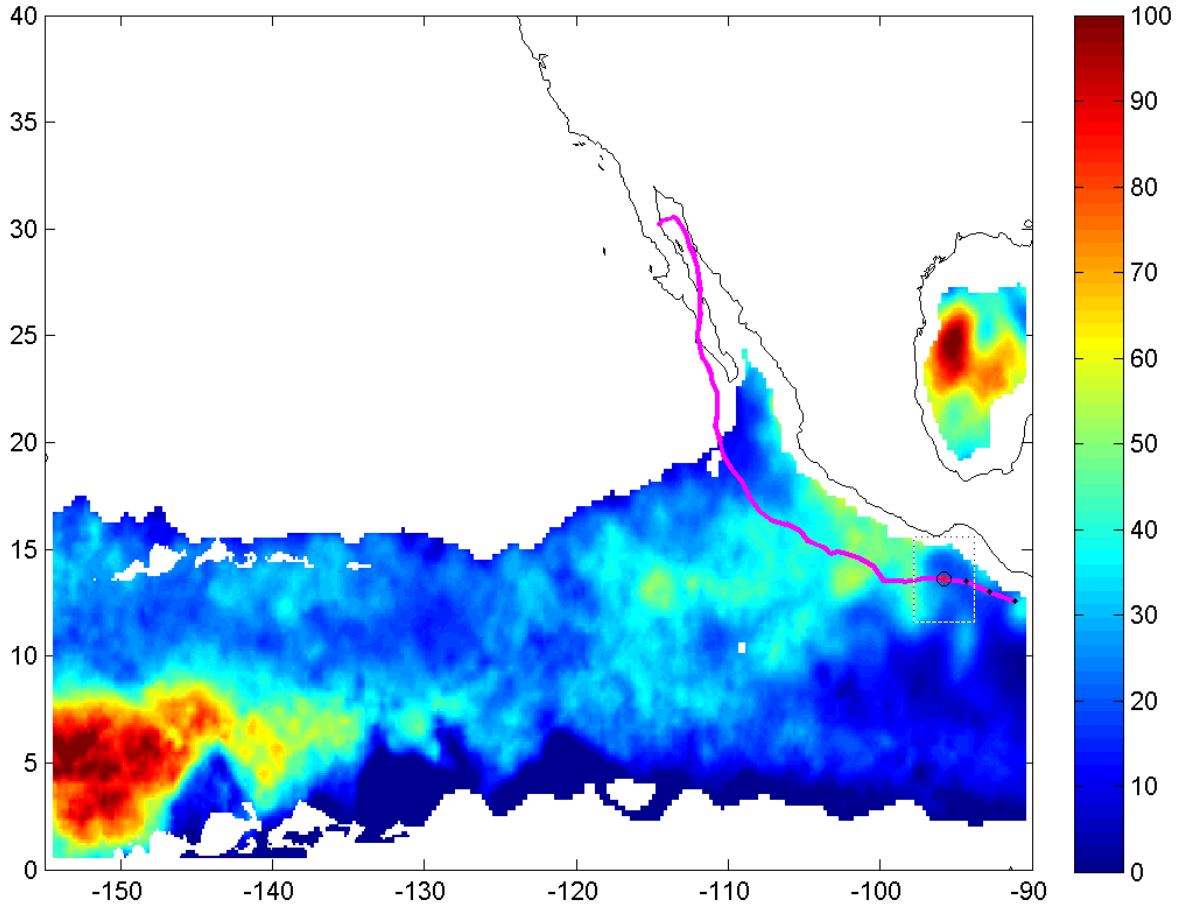

Figure 8: Ocean Heat Content (kJ cm^{-2}) calculated by the two-layer model approach, using SSHA data from AVISO and SST from TMI for hurricane Juliette at 0000 UTC 22 September 2001, few hours before its interaction with a region of locally enhanced Ocean Heat Content due to the presence of an Anticyclonic Ocean Eddy. The magenta line shows the complete hurricane trajectory, the black dots show the partial trajectory, the circled red asterisk shows the current position of the hurricane. The dashed line shows the 4° by 4° box used to calculate the mean value for the time series.

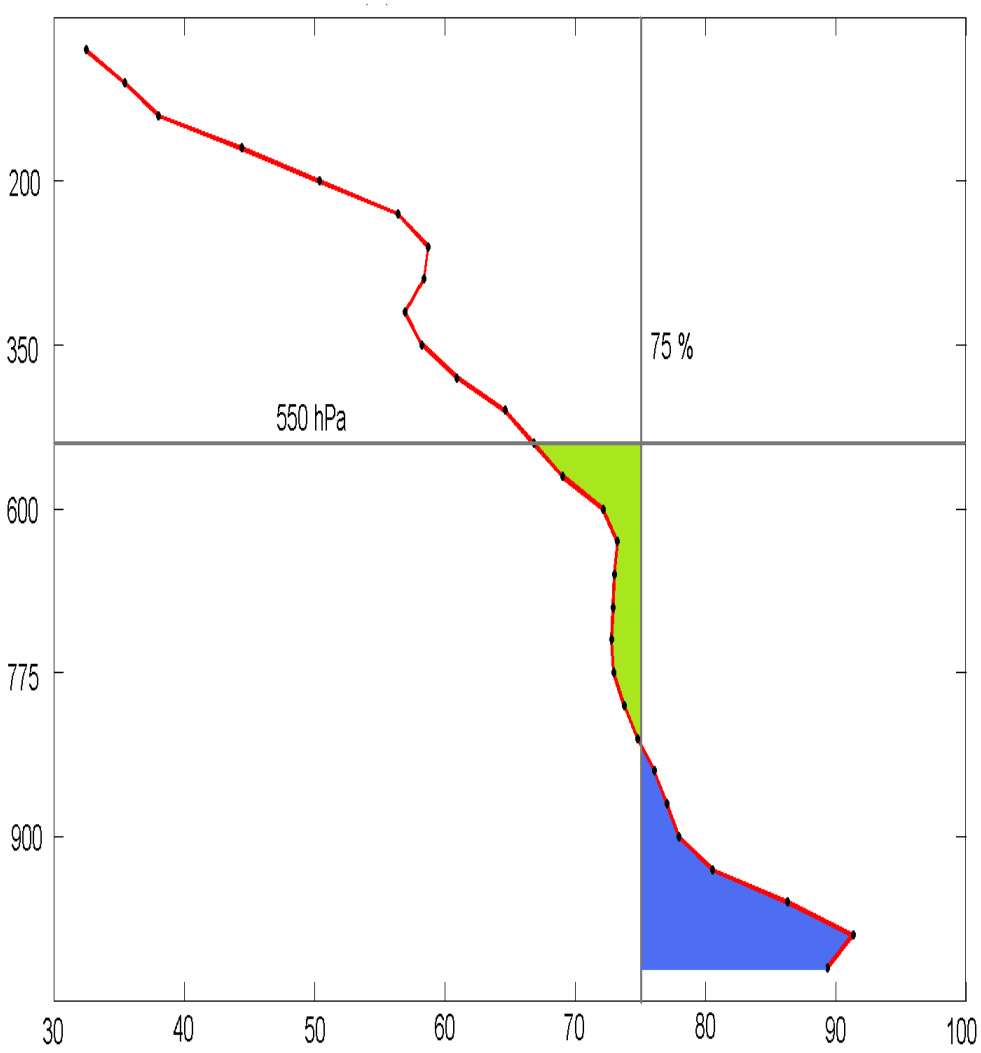

Figure 9: Relative humidity (%) profile and its integrated values from 550 to 1000 hPa levels with respect to a reference value of 75% relative humidity, calculated from NARR for hurricane Adolph at 0000 UTC 30 May 2001. The green area indicates dry air (with RH less than 75%) and the blue area indicates humid air (RH higher than 75%) in the environment surrounding the hurricane.

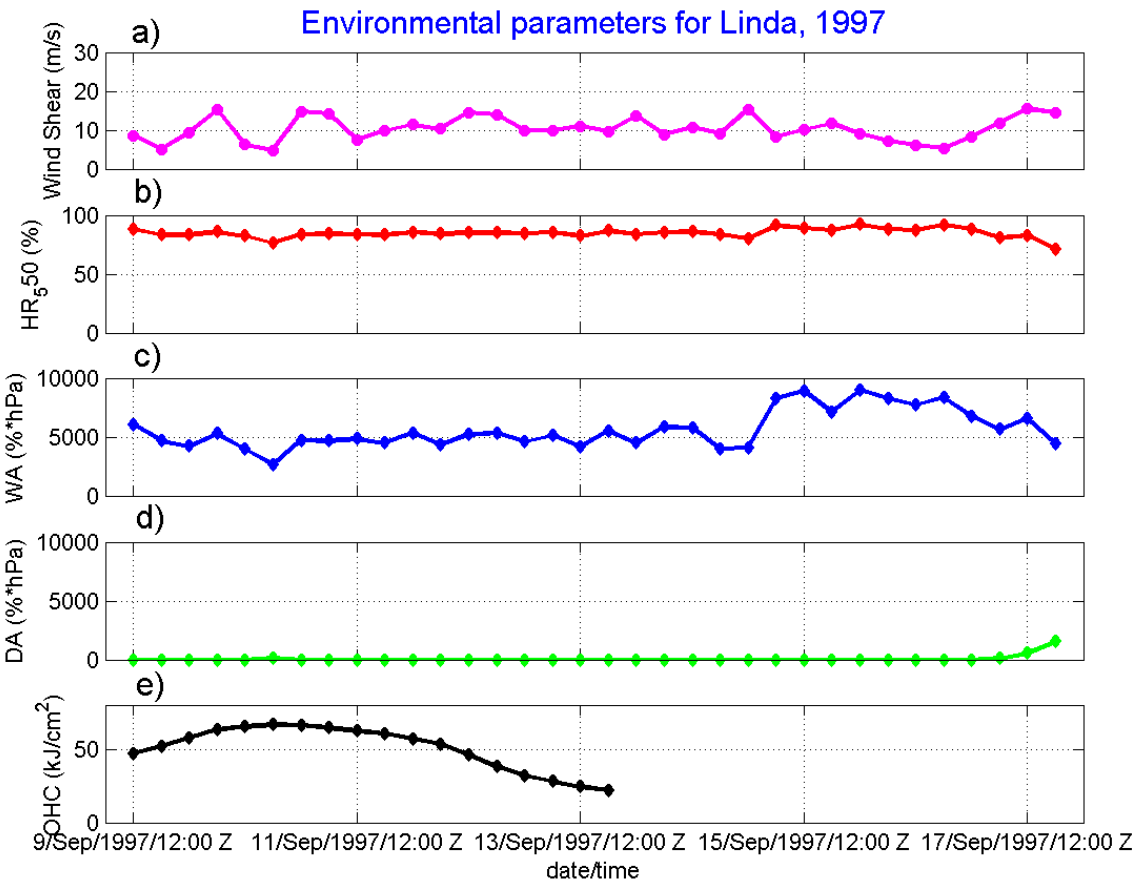

Figure 10: Time series for a) vertical wind shear (ms^{-1}), b) Relative Humidity at 550 hPa (%), c) vertically integrated humid air (%*hPa), d) vertically integrated dry air (%*hPa), and e) Ocean Heat Content (kJ cm^{-2}) for hurricane Linda, the most intense hurricane ever recorded in the NETP.

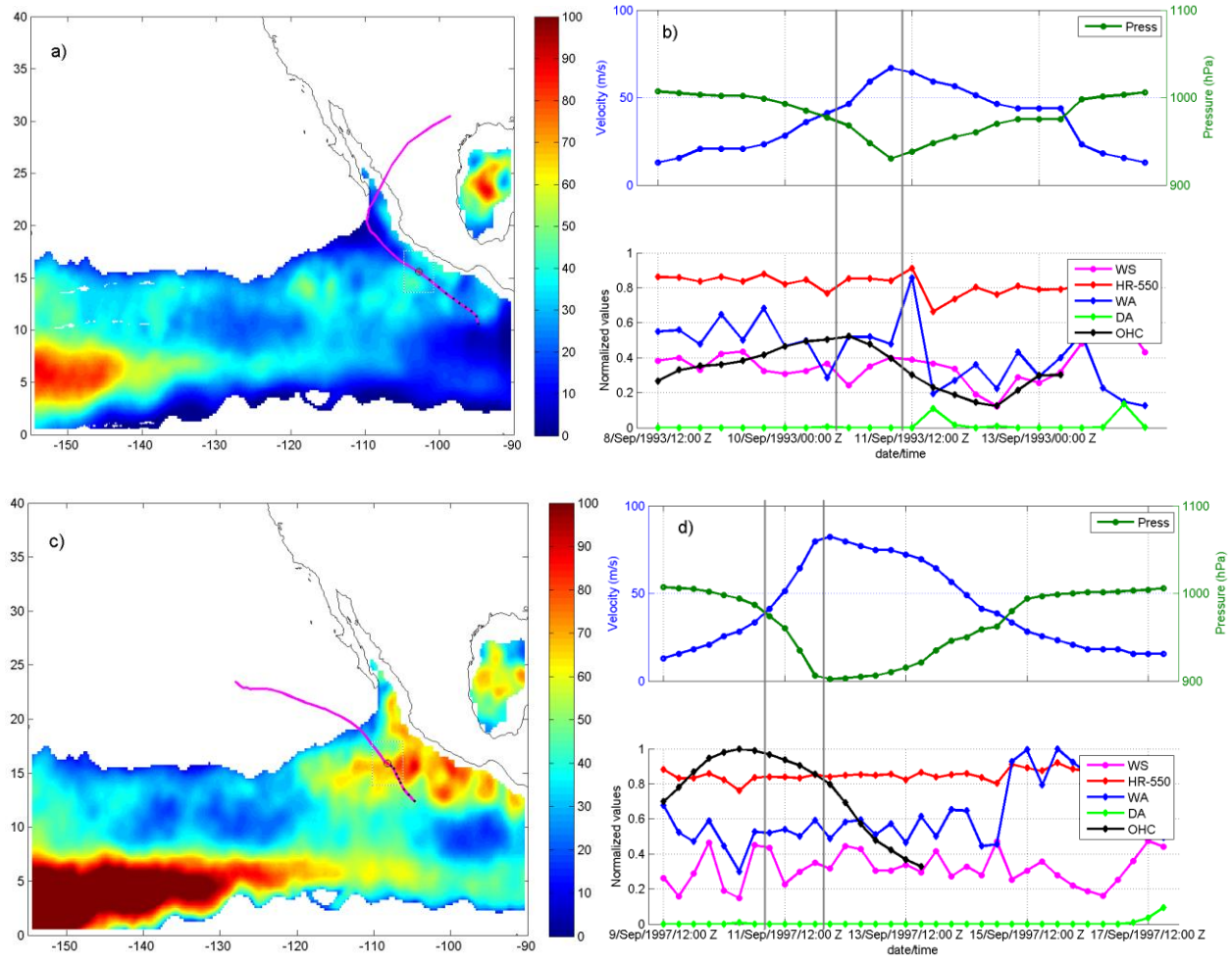

Figure 11: Objectively analyzed instant field of Ocean Heat Content (kJcm^{-2}) and Best-Track trajectory for hurricanes a) Lidia (1800 UTC 10 September 1993) and c) Linda (1200 UTC 11 September 1997) during its interaction with enhanced OHC by the presence of AOE. Time series for wind velocity (upper panel, blue line, left size scale) and pressure (upper panel, green line, right size scale) and normalized time series of RH at 550 hPa (bottom panel, red line), vertical wind shear 850-200 hPa (bottom panel, magenta line), dry air intrusion (bottom panel, green line) and moist air intrusion (bottom panel, blue line) and Ocean Heat Content evolution (bottom panel, black line) for b) Lidia-1993 and d) Linda-1997. The gray vertical lines in (b) an (d) highlight the Rapid and Explosive Deepening periods for each hurricane.

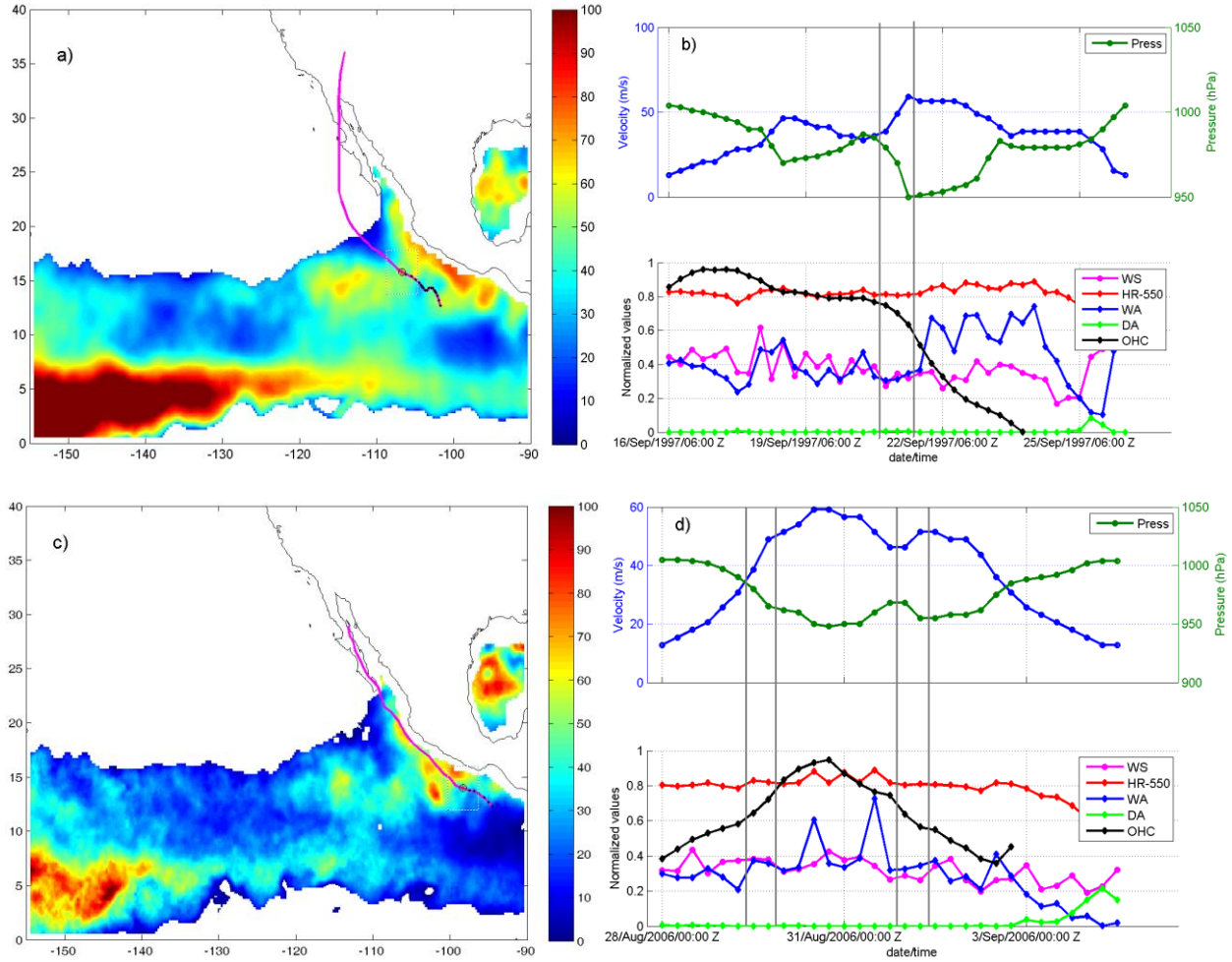

Figure 12: Objectively analyzed instant field of Ocean Heat Content (kJcm^{-2}) and Best-Track trajectory for hurricanes a) Nora (0000 UTC 21 September 1997) and c) John (1200 UTC 29 August 2006) during its interaction with enhanced OHC by the presence of AOE. Time series for wind velocity (upper panel, blue line, left size scale) and pressure (upper panel, green line, right size scale) and normalized time series of RH at 550 hPa (bottom panel, red line), vertical wind shear 850-200 hPa (bottom panel, magenta line), dry air intrusion (bottom panel, green line) and moist air intrusion (bottom panel, blue line) and Ocean Heat Content evolution (bottom panel, black line) for b) Nora-1997 and d) John-2006. The gray vertical lines in (b) an (d) highlight the Rapid Deepening period for each hurricane.

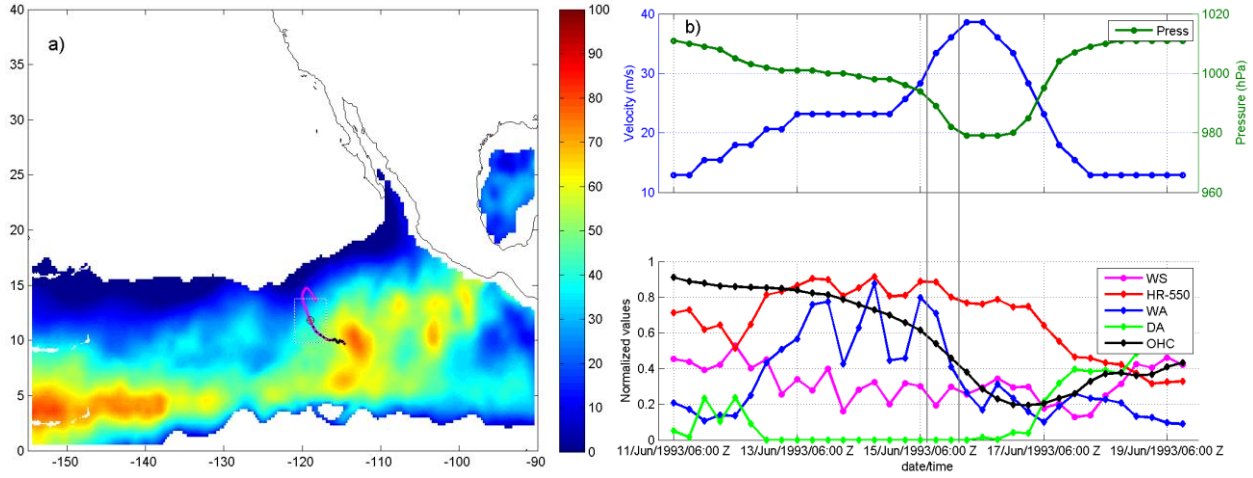

Figure 13: a) Objectively analyzed instant field of Ocean Heat Content (kJcm-2) and Best-Track trajectory for hurricane Adrian (1200 UTC 15 June 1993) b) time series for wind velocity (upper panel, blue line, left size scale) and pressure (upper panel, green line, right size scale) and normalized time series of RH at 550 hPa (bottom panel, red line), vertical wind shear 850-200 hPa (bottom panel, magenta line), dry air intrusion (bottom panel, green line) and moist air intrusion (bottom panel, blue line) and Ocean Heat Content evolution (bottom panel, black line) for hurricane Adrian. The gray vertical lines in (b) highlight the most important period of deepening for the hurricane.

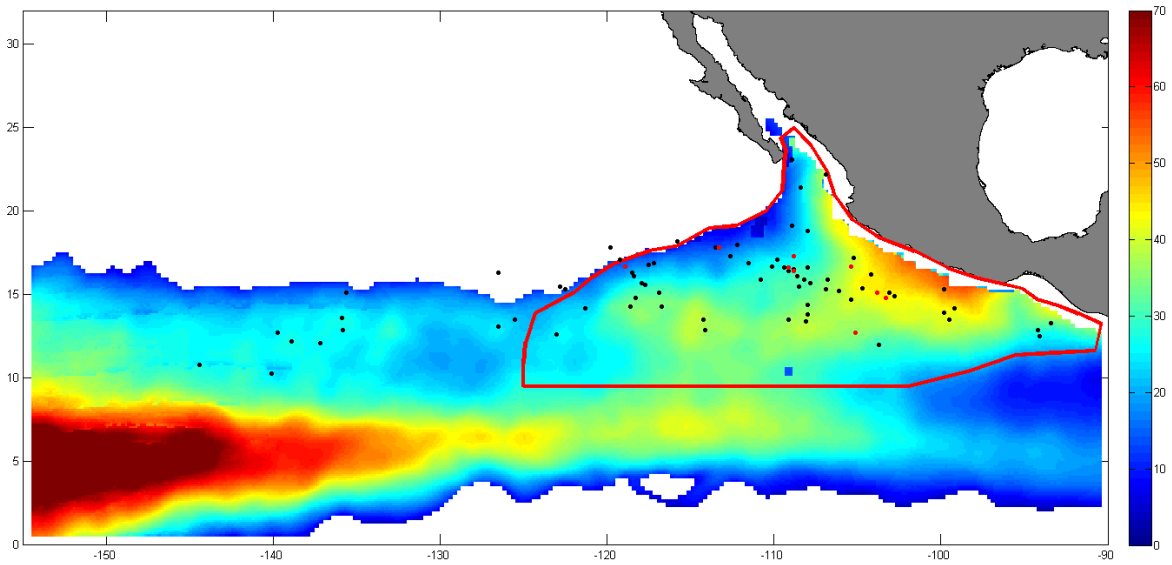

Figure 14: Composite mean OHC map (KJcm^{-2}) for all the analyzed cases that experienced RD or ED. The red line delimits the Main Favorable Ocean Region (MFOR) for the Northeastern Tropical Pacific basin. The dots indicate the locations where the analyzed hurricanes experienced Rapid Deepening (black dots) or Explosive Deepening (red dots). Note that a single hurricane may experience more than one episode of rapid or explosive deepening.

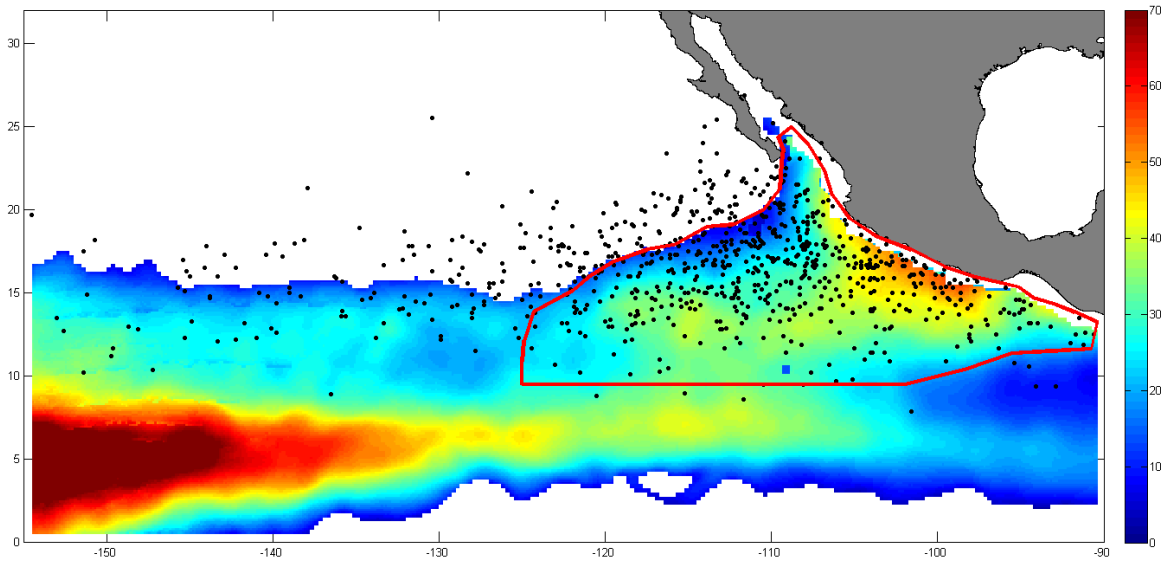

Figure 15: Same composite OHC map (KJcm^{-2}) as in Fig. 15. The red line delimits the Main Favorable Ocean Region (MFOR) for the Northeastern Tropical Pacific basin. The black dots show the positions where all the named tropical cyclones in the dataset (1949-2008) reached their maximum intensity. Note that 64% are located within the MFOR.

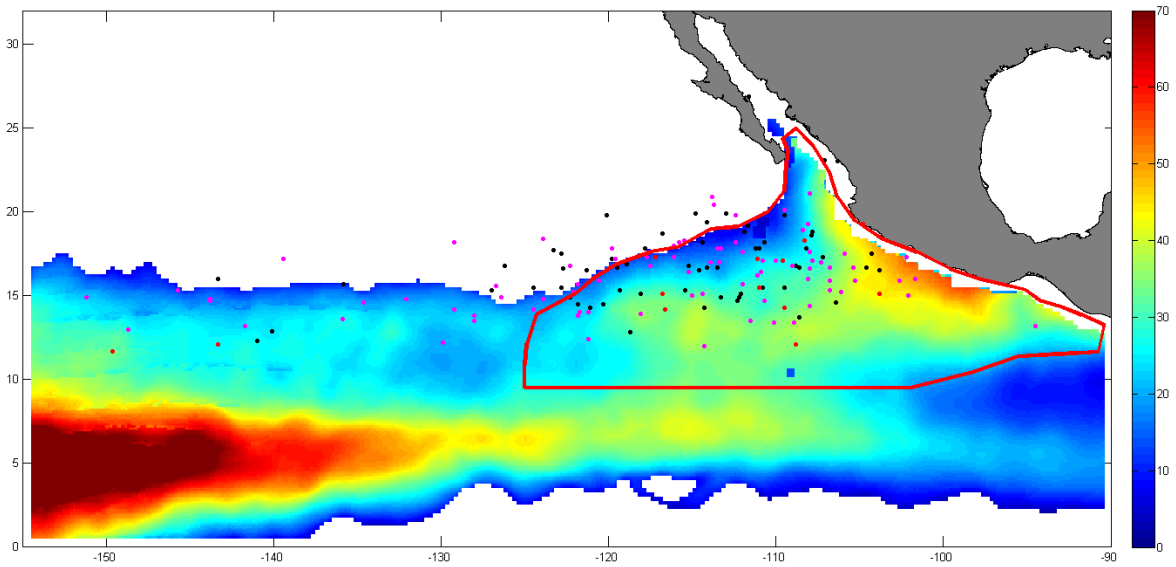

Figure 16: Same composite mean OHC map (KJcm^{-2}) as in Fig. 15. The red line delimits the Main Favorable Ocean Region (MFOR) for the Northeastern Tropical Pacific basin. The dots indicate the locations where all the hurricanes with category 3 (black), 4 (magenta) and 5 (red) in the full dataset (1949-2008) reached their maximum intensity.